Brain Stimulation 12 (2019) 110–118

Contents lists available at ScienceDirect

Brain Stimulation

journal homepage: http://www.journals.elsevier.com/brain-stimulation

EEG-triggered TMS reveals stronger brain state-dependent modulation of motor evoked potentials at weaker stimulation intensities

Natalie Schaworonkow [a, b], Jochen Triesch [a], Ulf Ziemann [b, *], Christoph Zrenner [b]

[a] Frankfurt Institute for Advanced Studies, Johann Wolfgang Goethe University, Frankfurt am Main, Germany
[b] Department of Neurology & Stroke, and Hertie Institute for Clinical Brain Research, University of Tübingen, Germany

ARTICLE INFO

Article history:
Received 21 January 2018
Received in revised form
7 September 2018
Accepted 15 September 2018
Available online 21 September 2018

Keywords:
EEG-TMS
Brain-state dependent brain-stimulation
Sensorimotor μ-rhythm
Corticospinal excitability
Motor evoked potential
Input-output curve

ABSTRACT

Background: Corticospinal excitability depends on the current brain state. The recent development of real-time EEG-triggered transcranial magnetic stimulation (EEG-TMS) allows studying this relationship in a causal fashion. Specifically, it has been shown that corticospinal excitability is higher during the scalp surface negative EEG peak compared to the positive peak of μ-oscillations in sensorimotor cortex, as indexed by larger motor evoked potentials (MEPs) for fixed stimulation intensity.
Objective: We further characterize the effect of μ-rhythm phase on the MEP input-output (IO) curve by measuring the degree of excitability modulation across a range of stimulation intensities. We furthermore seek to optimize stimulation parameters to enable discrimination of functionally relevant EEG-defined brain states.
Methods: A real-time EEG-TMS system was used to trigger MEPs during instantaneous brain-states corresponding to μ-rhythm surface positive and negative peaks with five different stimulation intensities covering an individually calibrated MEP IO curve in 15 healthy participants.
Results: MEP amplitude is modulated by μ-phase across a wide range of stimulation intensities, with larger MEPs at the surface negative peak. The largest relative MEP-modulation was observed for weak intensities, the largest absolute MEP-modulation for intermediate intensities. These results indicate a leftward shift of the MEP IO curve during the μ-rhythm negative peak.
Conclusion: The choice of stimulation intensity influences the observed degree of corticospinal excitability modulation by μ-phase. Lower stimulation intensities enable more efficient differentiation of EEG μ-phase-defined brain states.

Introduction

Oscillatory rhythms are a salient feature of brain dynamics [1,2] and are thought to organize cortical responses [3–5]. They have been shown to modulate cortical processing and influence perception and behavior. For instance, using correlative approaches, it has been found that the oscillatory phase of the sensorimotor rhythms modulates perceptual thresholds and behavioral responses [6–10]. When using transcranial magnetic stimulation (TMS), estimation of EEG-defined brain-state at the time of stimulation is methodologically challenging, because the large stimulation artefact prevents use of standard signal processing methods (e.g. band-pass filtering) which require a window of data both before and after the time point of interest. Additionally, evaluation of motor evoked potential (MEP) amplitude modulation by EEG phase requires a substantial number of trials per phase bin to achieve sufficient statistical power due to the well-known large inter-trial variability of MEP amplitudes [11,12]. These difficulties may partially explain why reports regarding the relationship between prestimulation phase and MEP amplitudes in the literature have been contradictory, either advocating for a clear relationship between prestimulation phase over sensorimotor areas and MEP amplitudes [10,13] or no relationship between prestimulation phase and MEP amplitudes [14,15].

Real-time EEG-triggered TMS enables the functional consequences of different brain states to be probed in a causal manner and increases statistical power by preferentially targeting specific oscillatory phases. In the context of the motor system, a recent study [16]

* Corresponding author.
E-mail address: ulf.ziemann@uni-tuebingen.de (U. Ziemann).

https://doi.org/10.1016/j.brs.2018.09.009
1935-861X/

demonstrated a dependence of corticospinal excitability and plasticity on the phase of the cortical μ-rhythm using a real-time triggered EEG-TMS system. The μ-rhythm is a prominent rhythm in the 8–13 Hz frequency band that can be recorded over central and motor electrodes, with a topography distinct from the α-rhythm. Similar to the α-rhythm, it is most pronounced in an idling state [17]. Subsequently, its oscillatory power and phase are referred to as μ-power and μ-power. Larger MEP amplitudes were elicited by TMS triggered at time of μ-rhythm surface negative peak (N) compared to μ-rhythm surface positive peak (P). In that study, a fixed stimulation intensity (eliciting MEPs of on average of 1 mV peak-to-peak amplitude or using a fixed stimulus intensity of 120% of MEP threshold) was used to examine the effects of ongoing brain activity on corticospinal excitability.

The present study is motivated by the belief that the identification and characterization of functionally relevant EEG-defined large-scale brain-states is of critical importance for the development of more stable and effective personalized EEG-modulated therapeutic brain-stimulation protocols. The goal is to investigate the conditions under which functionally differentiable brain-states can be optimally identified in EEG-triggered TMS, specifically with regard to stimulus intensity.

Our recent computational modelling work suggests a larger relative excitability modulation by phase for lower stimulation intensities [18]. Here, we experimentally addressed the question of which stimulation parameters are optimal for the differentiation of μ-rhythm derived brain states. We investigated how μ-phase-modulation of corticospinal excitability changes as a function of stimulation intensity. Using a real-time EEG-TMS set-up, pulses of five different stimulation intensities were triggered at two different oscillatory phase states (positive and negative peak) of the ongoing sensorimotor μ-rhythm, while MEPs were obtained to measure corticospinal excitability in each phase and intensity condition.

Materials and methods

Participants

The study protocol conformed to the Declaration of Helsinki and was approved by the local ethics committee at the medical faculty of the University of Tübingen (protocol 716/2014BO2). Written informed consent was obtained from all participants prior to the experiment. 17 right-handed participants (5 male, 12 female, mean age: 25.4 ± 2.6 years, age range: 22–32, average laterality score in Edinburgh handedness survey: 0.90 ± 0.12) with no history of neurological disease and usage of CNS drugs were selected from a pre-screened participant pool based only on the following inclusion criteria: (1) RMT of right abductor pollicis brevis (APB) or first dorsal interosseous (FDI) muscle $\leq$ 62.5% of maximum stimulator output (MSO), so that a stimulation intensity range of up to 160% MSO (1.6*62.5% = 100% MSO) could be explored. (2) The presence of a μ-rhythm with sufficient signal-to-noise ratio (SNR), as an adequate SNR is required for the phase-detection algorithm to estimate phases with sufficient accuracy. SNR was evaluated as follows (similar to Nikulin and Brismar [19]): A power function ($c \cdot x^{\alpha}$) was fitted to the 1/f noise of the resting EEG data power spectrum from Laplace-filtered C3-electrode of each individual participant. For that, data points from frequency bins with typically no oscillatory components present (0.5–8 Hz, 30–40 Hz) were used. The fitted noise was subtracted from the power spectrum. The adjusted power in the 8–13 Hz band was assessed for a clearly identifiable peak in the μ-range, with 5 dB over noise level as inclusion threshold. Two participants were excluded from the experiment, one because of excessive pre-innervation in the EMG (with 54.1% of trials discarded according to the predefined threshold criterion), the other because the MEPs evoked by the fitted intensities for phase-dependent stimulation differed greatly (by 98.4%) from the IO curve fitted on median MEPs recorded in the pre-experiment, likely due to a coil position mismatch. This resulted in a sample size of 15 participants. Experiments were performed in accordance with current TMS safety guidelines [20]. All participants tolerated the procedures without any adverse effects.

Experimental set-up

EEG and EMG recordings

A combined EEG-TMS set-up was used to trigger stimulation pulses according to the instantaneous oscillatory phase of the recorded μ-rhythm. Scalp EEG was recorded from a 64-channel TMS compatible Ag/AgCl sintered ring electrode cap (EasyCap GmbH, Germany) in the international 10–20 system arrangement. Scalp electrode preparation consisted of light skin abrasion followed by filling with conductive gel (Electrode Cream, GE Medical Systems, USA) until an impedance of <5 kΩ was reached. A 24-bit biosignal amplifier was used for combined 64-channel EEG and 2-channel EMG recordings (NeurOne Tesla with Digital Out Option, Bittium Biosignals Ltd., Finland), data were acquired in DC mode with a sample rate of 80 kHz at the head-stage and down-sampled online to a sample rate of 5 kHz. EMG was recorded from relaxed right APB and FDI muscle with bipolar adhesive hydrogel electrodes (Kendall, Covidien) in a belly-tendon montage (active amplifier input on the muscle belly and the reference input on the distal tendon (proximal interphalangeal joint)).

TMS set-up

A passively cooled TMS double coil (PMD70-pCool, 70 mm winding diameter, MAG & More GmbH, Germany) was used together with a magnetic stimulator (Research 100, MAG & More GmbH, Germany) configured to deliver biphasic single cosine cycle pulses with 160 μs period such that the second phase of the biphasic pulse induced an electrical field from lateral-posterior to medial-anterior, i.e., orthogonal to the central sulcus. Each TMS pulse was individually triggered through an external trigger input from the real-time system. Stimulation intensity was set programmatically using an analog control interface between 0 and 5 V and corresponding to 0–100% of maximum stimulator output through an analog output port interface (UEI PD2-MF-64-500/16L, United Electronic Instruments, USA) from the real-time system to allow for randomized ordering of intensity conditions. Stimulation was applied to the hand representation of left primary motor cortex (M1). The motor hot spot was identified as the coil position and orientation resulting consistently in maximum MEP amplitudes [21]. The target muscle was the muscle which responded to the lowest stimulator intensity and was then subsequently used to determine resting motor threshold (RMT) as the lowest intensity that elicited MEPs with a peak-to-peak amplitude of at least 50 μV in 5 out of 10 trials [22]. A neuronavigation system (Localite GmbH, Sankt Augustin, Germany) was used to mark the coil position over the motor hot spot to monitor coil stability over time.

Real-time EEG-triggered brain stimulation

The real-time processing system used in this experiment is described in detail in Zrenner et al. [16]. Briefly, an algorithm implemented in Simulink Real-Time (Mathworks Ltd, USA, R2016a) was used for real-time data acquisition, data processing and as the TMS stimulator control system. The algorithm was executed on an xPC Target processor (DFI-ACP CL630-CRM mainboard), processing online EEG data streamed through a real-time ethernet interface from the Digital Out interface of the EEG main unit in data packets at a rate of 1 kHz. The EEG signal used for real-time triggering was comprised of EEG channels overlying left sensorimotor cortex (C3,

CP1, CP5, FC1, FC5), which were combined in a C3-centered Laplacian montage [23]. Data were down-sampled to 1 kHz by averaging and a sliding window of data of 500 ms width was used to compute estimates of instantaneous phase. The signal window was bandpass filtered (finite impulse response filter with order 128 and pass band 8–12 Hz), the last 64 ms were discarded because of edge artefacts and then forward predicted by an autoregressive model (Yule-Walker, order 30) for 128 ms. The analytic signal was computed by fast Fourier transform-based Hilbert transform, which was used to determine the instantaneous phase. In addition, the power spectrum was calculated from a sliding window of 1024 samples using Hann-windowed FFT and integrating spectral power in the 8–12 Hz frequency band. A digital output signal was generated to trigger the magnetic stimulator when three conditions were met: (1) an interstimulus interval (ISI) to the preceding pulse larger than 1.5 s (2) the temporal evolution of the phase estimate crosses the target phase. (3) a predefined μ-power threshold is met. The power-threshold was adjusted on an individual participant basis at the beginning of the experiment such that a median ISI of 2 s resulted. In the case of random-phase stimulation, only the minimum ISI and μ-power were considered as conditions for triggering the magnetic pulse, and a random delay was imposed between 0 and 100 ms.

Experimental session

The experimental session consists of three types of blocks, as illustrated in Fig. 1a: (1) Resting state EEG recordings were made, with eyes open and closed (5 min eyes open, participants instructed

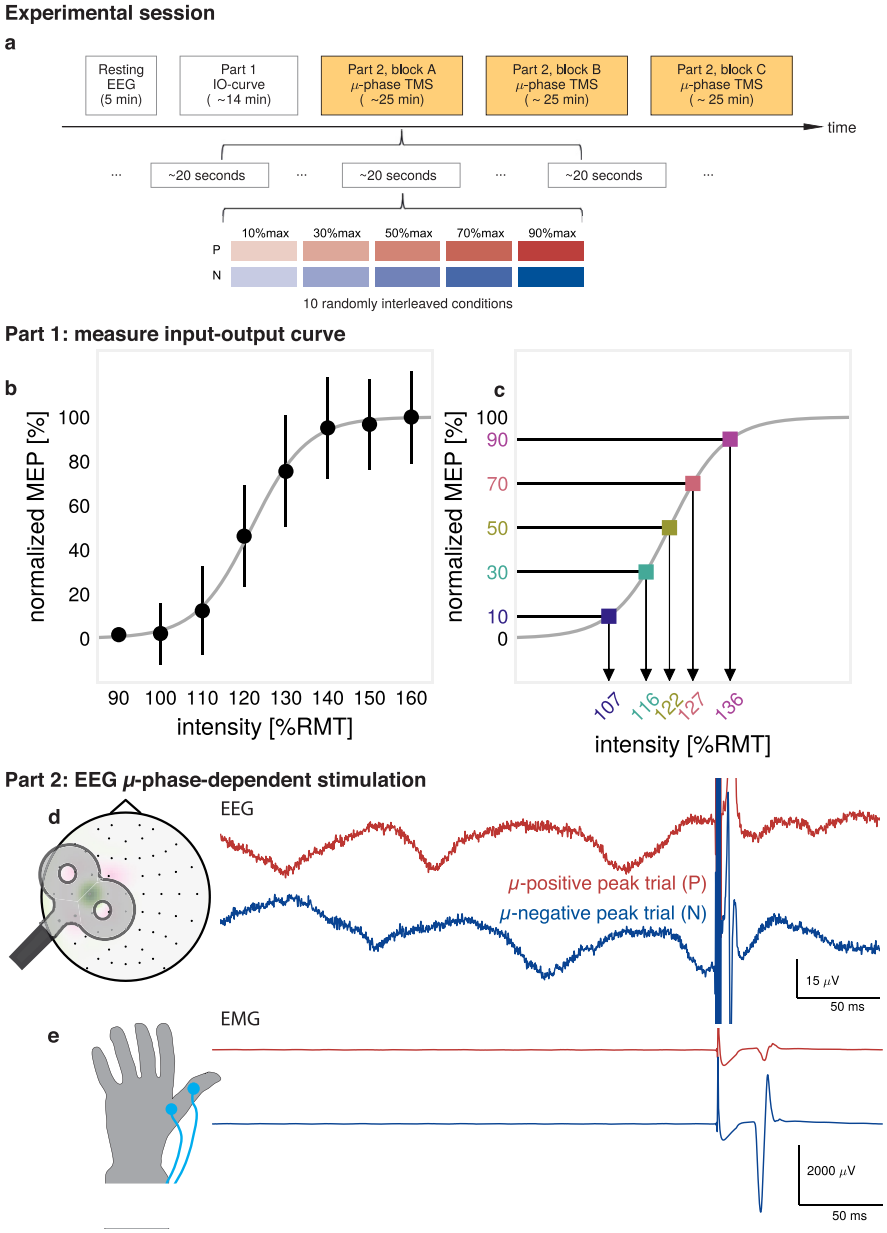

Fig. 1. Experimental Session. (a) Timeline of the experimental session. In each μ-phase TMS block, ten randomly interleaved conditions were tested, P– and N-trials for five intensities. (b) An IO curve is determined from phase-independent stimulation. Shown is an example IO curve for a single participant. A logistic function (grey curve) is fitted on median MEPs (black circles). Error bars indicate ±1 SD. (c) From the logistic fit, five intensities (colored squares) are chosen for phase-dependent stimulation. (d) EEG μ-phase-triggered stimulation is performed, according to the instantaneous phase from the Laplace-filtered C3-signal. Two example single trials for the two types of trigger conditions, surface positive μ-peak (P) and surface negative μ-peak (N). (e) The corresponding single-trial EMG signals recorded for the two trigger conditions, with MEPs in the interval 20–40 ms after stimulation.

to fixate cross 1 m in front of participant, followed by 1 min eyes closed). (2) An IO curve was obtained (Fig. 1b). Eight intensities (90%–160% RMT, in steps of 10%) were tested in randomized order, with 40 pulses per condition, applied with random-phase stimulation. The median ISI was 1.92 ± 0.24 s across participants. The IO curve was fitted with a logistic function $f(s) = 1/(1 + \exp(-b \cdot (s-a)))$. Five stimulation intensities were chosen on the individual IO curve where median MEP amplitudes resulted at the following percentages of the maximum saturation level: $SI_{10\% max}/SI_{30\% max}/SI_{50\% max}/SI_{70\% max}/SI_{90\% max}$ (Fig. 1c). The average length of the IO curve session was 14 min (3) μ-phase-triggered stimulation with real-time EEG-triggered TMS at surface μ-positive peak and surface μ-negative peak conditions was performed at the five intensities chosen in the previous block in randomized order with 60 pulses per condition (Fig. 1d), resulting in 600 pulses per block. The average length of this block was 25 min. The phase-dependent stimulation block was repeated three times, i.e., 2 phases × 5 intensities × 60 pulses × 3 blocks = 1800 pulses total. Between blocks, subjects were allowed a break, the length was dependent on subject comfort level (average break duration: 9 min). We have chosen a stimulus frequency of 0.5 Hz in order to maximize the number of trials within the time available. Plasticity effects may be induced at this frequency. However, this is mitigated by the interleaved conditions experimental design, which ensures that any time effects will affect all experimental conditions to the same degree. The stimulator intensity was automatically adjusted between pulses, intensity conditions were applied in randomized order. Between phase-dependent pulses, the median ISI was 1.92 ± 0.15 s across participants. Median ISI before P-trials was 1.93 ± 0.15 s across participants, and 1.93 ± 0.16 s across participants before N-trials. Within-subject comparison between P– and N-trial ISI distributions with a Wilcoxon rank-sum test was not significant ($p > 0.05$) in any subject. As an output measure, EMG was recorded (Fig. 1e). Including preparation, the average total length of the experimental session amounted to 4 h (±20 min).

Data analysis and statistics

Data were analyzed with Matlab (Mathworks Ltd, USA, R2017b) and the BBCI toolbox [24]. EMG signals were high-pass filtered (Butterworth, filter order 2, 10 Hz). Trials with muscle activity 500 ms before stimulation onset were discarded with a threshold criterion (max-min amplitude > 50 μV). Peak-to-peak MEP amplitudes were determined within the interval of 20–60 ms after TMS pulse. All MEP time courses were inspected manually. A threshold of 50 μV was chosen as a cut-off for EMG responses so that the peak-to-peak amplitude can be determined reliably. In order to minimize the number of non-response trials and to avoid the difficulty of quantifying very small EMG potentials, we have chosen stimulus intensities above RMT only. The statistics were performed both with setting the non-responses to zero and excluding the non-responses entirely in order to validate that the small number of expected non-responses did not affect the overall result. Trials of the three phase-dependent blocks were pooled. For one participant, the last phase-dependent block was discarded because of excessive coil drift. The C3-centered EEG-Laplace filter extracted μ-rhythm pre-stimulation activity (500 ms before stimulation) was manually inspected for artefacts, and corresponding trials were discarded. Overall, 7.8% of trials were discarded for the phase-dependent stimulation sessions.

According to our computational I-wave model [18], the IO-curve shifts to the left for N-trials relative to P-trials, see conceptual illustrations in Fig. 2a. The model is composed of a feedforward

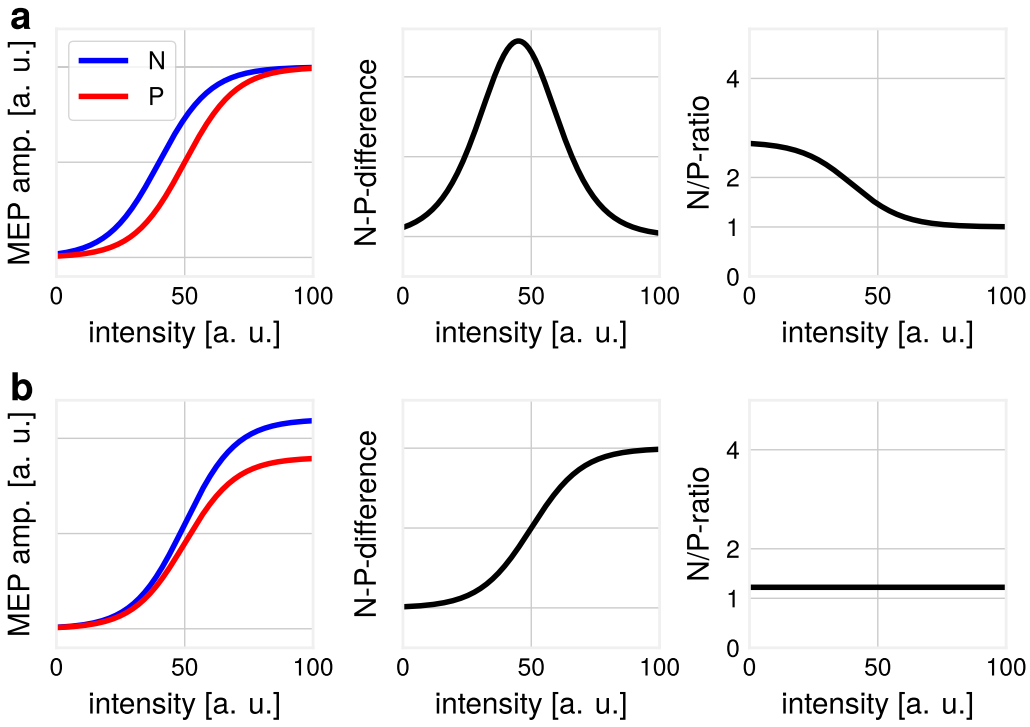

Fig. 2. Illustration of different simplified recruitment models on N/P-measures. (a) Vertical IO-curve shift: N–IO curve $f_N(s) = \frac{A}{1+\exp(-B \cdot (s-C_N))}$ vs. P–IO curve $f_P(s) = \frac{A}{1+\exp(-B \cdot (s-C_P))}$. The shift respective to the x-axis is given by parameter C, with $C_N < C_P$. The maximal amplitude is determined by the parameter A, and the steepness of the logistic function by parameter B. The differences in the shift parameter determine shapes of N/P-difference and N/P-ratio measures. (b) Increased gain for N-trials: N–IO curve $g_N(s) = \frac{A_N}{1+\exp(-B \cdot (s-C))}$ vs. P–IO curve $g_P(s) = \frac{A_P}{1+\exp(-B \cdot (s-C))}$, with the same shift value for shift parameter C and different maximal amplitudes, with $A_P < A_N$.

network of layer 2/3 and layer 5 neurons, with the layer 2/3 neurons receiving oscillatory input, which results in subthreshold oscillations in the layer 5 neurons. As the mean membrane potential of the layer 5 neurons at the time point of stimulation is therefore elevated for N-trials relative to P-trials, a larger response is seen on average for stimulation of the same intensity throughout the range of stimulation intensities, with a constant level of "neural noise" added by TMS [25]. Considering a high stimulation intensity, the impact of the background activity is small, compared to the stimulation pulse and conversely for a small stimulation intensity. This results in the largest absolute differences between MEPs of P− and N-trials for intermediate intensities and largest relative differences between MEPs of P− and N-trials for small intensities. While the MEP amplitudes reach a ceiling level for high intensities, there is still considerable variability in MEP amplitudes for high intensities, which makes a model like Fig. 2b conceivable, where N-trials result in a higher maximal amplitude of the IO-curve. A preferential recruitment of late I-waves in N-trials compared to P-trials could disproportionately influence the recruitment of α-motoneurons [26]. In this model, absolute differences between MEP amplitudes will be largest for large intensities and relative differences between P− and N-trials will be constant through the stimulation range.

Therefore, we evaluated the MEP differences with two measures, quantifying relative as well as the absolute MEP differences between N− and P-trials. We quantified the relative phase-modulation by calculating the ratio $\frac{\text{median}(\text{MEP}_\text{N})}{\text{median}(\text{MEP}_\text{P})}$ and the absolute phase-modulation by calculating $\frac{\text{median}(\text{MEP}_\text{N})-\text{median}(\text{MEP}_\text{P})}{\text{IOC}_\text{max}}$ for each intensity condition, respectively, where IOC_max is the median MEP evoked at intensity 160% RMT, measuring the individual IO curve saturation level. We assessed the effect of intensity on phase-modulation by bootstrapping. Trials were randomly partitioned (with replacement) into two classes and the ratio and difference measures were calculated. This procedure was repeated for 100 000 iterations to arrive at confidence bounds and p-values. Group effects were evaluated with a Wilcoxon signed-rank test on the N/P-ratios for each intensity condition, the significance level was Bonferroni-corrected. Due to the insensitivity to transformations, this test yields the same result for N/P-ratio and N/P-difference.

To illustrate the effect of the sample size on the probability of detecting a difference between N− and P-trials for every intensity condition we used a simulation approach. For each participant, MEPs were resampled with replacement separately for N− and P-trials for varying sample sizes. A Wilcoxon rank-sum test was performed, noting whether the null hypothesis was rejected. This procedure was repeated 10 000 times.

Results

Methodological efficacy

To estimate the accuracy of the real-time phase-trigger algorithm, we determined the instantaneous phase by passing the 5 min resting EEG through the Simulink model from the experimental session to determine time points at which the algorithm would trigger. This procedure was chosen to avoid contamination by stimulation artefacts. Instantaneous phase was estimated by using Hilbert transform on the Laplacian C3 signal and band-pass filtered in 8–13 Hz frequency range. Phase prediction accuracy (mean ± standard deviation) across participants was $-1.74^\circ \pm 53.65^\circ$ in the positive peak condition and $178.26^\circ \pm 55.67^\circ$ in the negative peak condition. Angular phase accuracy distribution plots for individual participants are shown in supplementary Fig. S1. The achieved phase accuracy was as expected similar to Zrenner et al. [16], as no changes were made to the core phase-detection algorithm.

To validate that the intensities chosen for the phase-triggered measurement session matched the section of the IO curve measured during the random-phase pre-measurement, the resulting averaged MEP amplitudes were compared by computing the percentile rank of the median MEP amplitude for phase-stimulation conditions, pooled across N− and P-trials, assuming median MEPs from random-phase stimulation reflect an average of N− and P-trials. We found a mean deviation of $-0.2\% \pm 12.0\%$, which allows adequate comparisons to the random-phase IO curve. The IO curves for individual participants can be found in supplementary Fig. S1e. Regarding effects on MEP amplitudes over time, there was no significant difference across subjects between medians of first and last 100 trials for each individual block, nor pooled across blocks (normalized by subject-specific median across whole experiment, Wilcoxon signed-rank test, $p > 0.05$).

Phase-modulation across stimulation intensity range

To illustrate the effect of μ-phase on MEP amplitudes, Fig. 3 shows data from one measurement session for an illustrative single participant, including the phase-dependent IO curves as well as MEP histograms, and the IO curve from the pre-experiment with random-phase stimulation. To quantify the effect of pre-stimulation μ-phase, we compared relative and absolute differences between MEP amplitudes of N− and P-trials.

The mean influence of stimulation intensity on the degree of MEP amplitude modulation by μ-phase across all participants is shown in Fig. 4. We replicated the dependence of MEP amplitude on phase of the sensorimotor μ-rhythm at the time of TMS (i.e., larger MEP amplitudes at the negative peak of the μ-rhythm) [16] and detected a significant difference between N− and P-trials in four out of five intensity conditions. The effect of stimulation intensity on modulation by μ-phase was assessed as relative and absolute differences between N− and P-trials. The mean N/P-ratio value is smaller for higher intensity, (Fig. 4b). MEP amplitudes at the μ-negative peak were on average between 101% (at $\text{SI}_{10\%\,\text{max}}$, corresponding on average to 105% RMT, $p = 0.006$, two-tailed Wilcoxon signed-rank test) and 8% (at $\text{SI}_{90\%\,\text{max}}$, corresponding on average to 138% RMT, $p > 0.05$) larger than MEPs evoked at the μ-positive peak. The N/P-difference peaked at the intermediate intensity $\text{SI}_{50\%\,\text{max}}$, with a group average difference between N− and P-trials of 10.5% of IOC_max (Fig. 4c). The measures for individual participants are shown in supplementary Figs. S2 and S3. For the participant with the largest observed N/P-ratio, the phase-dependent stimulation MEPs are lower compared to the random-phase stimulation IO curve (participant S16, supplementary Fig. S1e). This leads to larger N/P-ratio-values and to deviation from the N/P-ratio computed from the logistic fit (Fig. 4b). Variability of MEP amplitudes is higher at low intensities, as measured by the coefficient of variation (across participants, mean $\text{CV}_{10\%\,\text{max}} = 1.34$, $\text{CV}_{30\%\,\text{max}} = 0.81$, $\text{CV}_{50\%\,\text{max}} = 0.66$, $\text{CV}_{70\%\,\text{max}} = 0.53$, $\text{CV}_{90\%\,\text{max}} = 0.43$). Due to higher variability of MEP amplitudes at low intensities, even large N/P-ratio values are not always significant within participants according to the bootstrap test.

The results investigating the effect of number of trials in a simulation approach are shown in Fig. 5. Using 180 trials per condition, the mean probability to reject the null hypothesis (N/P-ratio equals 1 or N/P-difference equals 0) within a single participant is 62% for the $\text{CV}_{10\%\,\text{max}}$ and $\text{CV}_{30\%\,\text{max}}$ conditions, and around 35% for the $\text{CV}_{90\%\,\text{max}}$ condition. Using only 90 trials, these values decline to 50% and 28%, respectively. This demonstrates that the required number of trials to differentiate between μ-phase-defined states with high statistical power within participants can

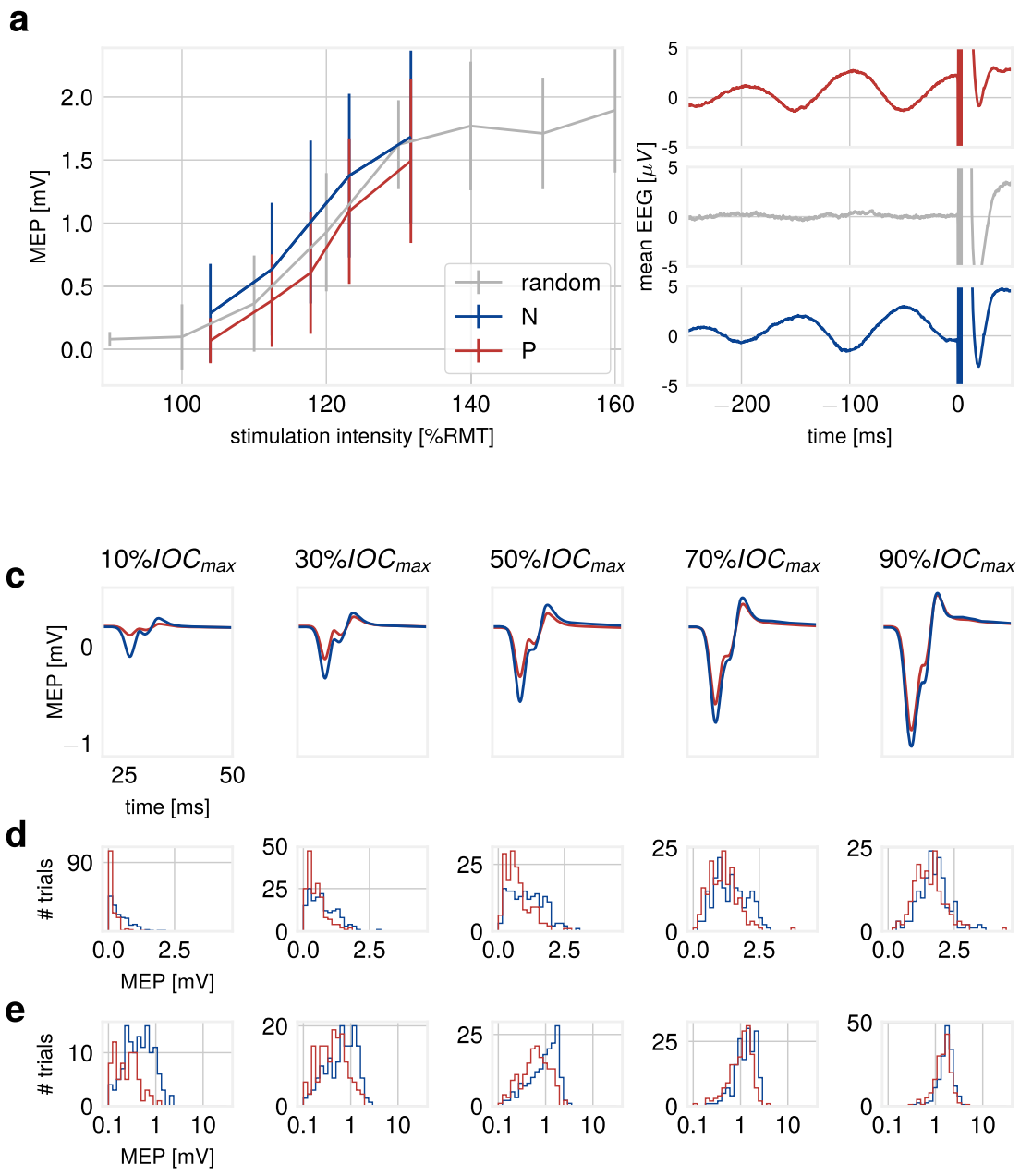

Fig. 3. Results for illustrative participant. (a) IO curve for phase-dependent stimulation. Stimulation at the μ-phase negative peak (N) evokes MEPs of larger amplitudes (blue curve) than stimulation at the μ-phase positive peak (P, red curve). The random-phase IO curve runs in between (grey curve). Error bars indicate ±1 SD. (b) Mean pre-stimulus C3 Laplacian-filtered EEG for N– and P-trials. (c) Mean MEP amplitudes (in mV) for the five stimulation intensities (blue: N-trials, red: P-trials) (d) Frequency distribution histograms of MEP amplitudes for the five stimulation intensity conditions on a linear scale (blue: N-trials, red: P-trials), non-responses excluded. (e) Histograms as in (d) but on a logarithmic scale to ease comparison at low intensity. (For interpretation of the references to color in this figure legend, the reader is referred to the Web version of this article.)

be reduced by choosing a lower stimulation intensity. In this analysis, all participants are included, as the goal of this analysis is to show relative differences in required sample sizes between intensities. For participants without observable modulation of MEP amplitudes by μ-phase, the null hypothesis may be true, therefore the actual statistical power at a given sample size is higher than the average probability of rejecting H_0. For instance, for the three participants showing the largest phase-modulation, only 14, 41 or 44 trials are required per condition (e.g. for the intensity SI = 30% max) to find a significant difference between N– and P-trials with a statistical power of 80%. At the group level, using a low to intermediate intensity will enable detection of significant effects of the size observed in the current study with high certainty.

Degree of observed MEP amplitude modulation

In our study, 13 out of 15 subjects displayed a N/P-ratio larger than 1 in at least four out of the five tested intensity conditions. The observed degree of MEP amplitude modulation by instantaneous μ-phase differed across subjects. We performed a number of correlation analyses in order to identify possible factors,

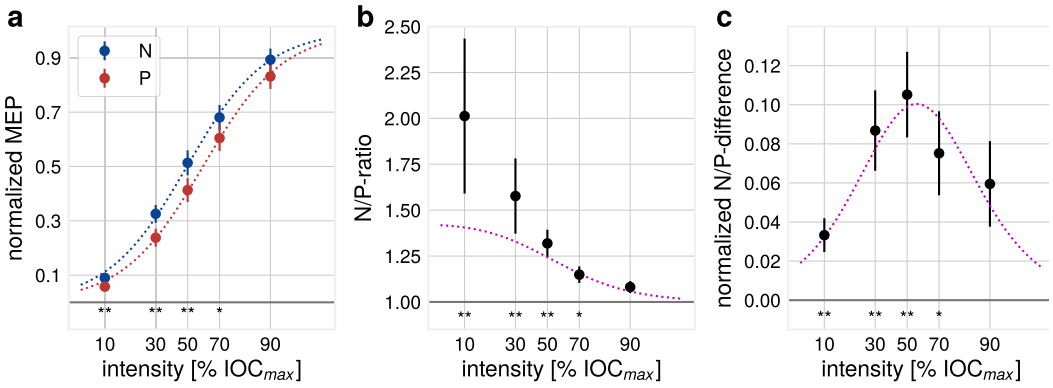

Fig. 4. Group level results. (a) IO curve, for N− and P-trials, normalized to IOC_{max}. A logistic function was fit to N− and P-trial median MEPs across intensity conditions separately (dotted lines). Error bars indicate ±1 SEM. P-values (Bonferroni-corrected) for Wilcoxon signed-rank test for a N/P-ratio different from 1 across participants: $^{**}p < 0.01$ for $SI_{10\%\,max}$, $SI_{30\%\,max}$ and $SI_{50\%\,max}$, $^{*}p < 0.05$ for $SI_{70\%\,max}$ and $p > 0.05$ for $SI_{90\%\,max}$. (b) Mean N/P-ratio between N− and P-trials across subjects. Dotted lines correspond to N/P-ratio values as calculated from the logistic fit. Error bars indicate ±1 SEM. (c) Mean N/P-difference between N− and P-trials across subjects. Normalized to IOC_{max}, Dotted lines correspond to N/P-difference values as calculated from the logistic fit. Error bars indicate ±1 SEM.

which—apart from stimulation intensity—may predict the degree of observed MEP amplitude modulation by μ-phase: We found no significant correlation between SNR as obtained from resting state EEG data and the effect size across at five tested intensities, respectively ($p > 0.05$, Spearman rank correlation). Overall, higher SNR resulted in improved performance of the phase-detection algorithm as measured by decreased standard deviation of the phase accuracy ($r = -0.67$, $p = 0.0081$, Spearman rank correlation), but pronounced rhythm with high SNR did not translate to a larger phase-modulation effect. A significant sub-population of participants remained that showed a clear μ-rhythm without exhibiting a clear phase-modulatory effect on MEP amplitude. Additionally, no significant correlation was observed between distance of coil to center electrode of the Laplacian filter and effect size at all five tested intensities, respectively ($p > 0.05$, Spearman rank correlation). In this study, a standard MNI brain model was used for navigation. In future studies with individual participant MRI anatomy additional factors could be investigated, such as the orientation of dipoles underlying the mean topography around the stimulation trigger (supplementary Fig. S1b), coil position and orientation relative to the central sulcus. Therefore, the factors required for observing μ-phase modulation of corticospinal excitability remain to be further elucidated.

Discussion

We replicated the finding that corticospinal excitability as measured by MEP amplitude is modulated by the phase of the ongoing μ-rhythm [16], with larger MEP amplitudes at the negative compared to the positive peak. Additionally, in agreement with predictions based on our modelling work [18], we demonstrated that the magnitude of the modulatory effect depends on stimulation intensity, with largest relative modulation for low intensities and largest absolute differences for intermediate stimulation intensities. The reduced modulatory influence of μ-rhythm at high stimulation intensities can be explained by saturation of the IO curves of MEPs. If stimulation intensity is sufficiently far above the motor threshold, any ongoing fluctuations of that threshold influence behavioral outcomes to a lesser degree and will result in smaller relative differences between N− and P-trials. This is compatible with many previous findings showing greatest sensitivity of MEP amplitude to intervention in the low and/or intermediate parts of the IO curve (e.g. Refs. [27–30]).

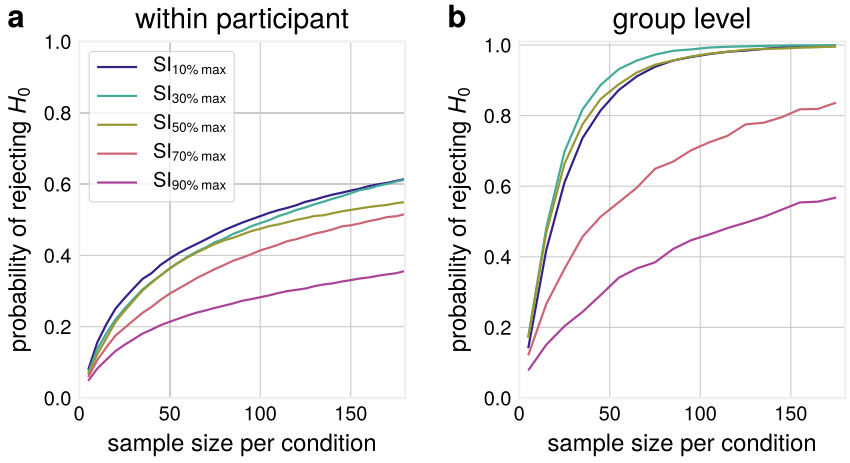

Fig. 5. Illustration of the effect of sample size on the probability of detecting a difference between N− and P-trials. The dependence of the probability to reject the null hypothesis of no difference between N− and P-trials on the used sample size for different stimulation intensities in (a) within participant comparisons and (b) group level comparisons (N = 15 participants included in this study).

Implications

This study investigates the optimal parameters (in terms of stimulus intensity) for investigating the broader neurophysiological question of the role of oscillatory brain-states and specifically how two putatively different states (such as negative vs. positive peak of the μ-rhythm) may be differentiated by their effect on state-triggered stimulus evoked responses. Whether the result, that weaker stimulus intensities enable better effective discrimination between putatively different states generalizes to other stimulus modalities (visual, auditory, tactile), remains to be investigated.

One practical implication of the present findings is that studies seeking to demonstrate differential EEG-defined brain states based on differential TMS-evoked responses should be designed with a sufficient number of interleaved trials (more than 100 per condition) and use low stimulation intensity to maximize statistical power, where the lower limit of intensity is determined by the proportion of non-responses and measurement noise when quantifying small responses. Based on this study, the intensity setting resulting in an average MEP amplitude 20% of IOC_{max} would be recommended; in our dataset, this corresponded to a stimulus intensity of on average 112% RMT, with 10 of the 15 participants in our sample in the range between 108 and 117 %RMT. However, depending on the IO curve, a stimulation intensity based on a fixed RMT percentage can already be in the saturation range of an individual participant, where MEP amplitudes do not significantly differ between μ-phase conditions. Conversely, in our study the median MEP amplitudes for high stimulation intensity ranged from 0.6 to 10.9 mV across participants. A stimulation intensity based on a fixed MEP amplitude such as 1 mV can also be in the saturation range for an individual subject. Measuring the individual IO curve and specifically estimating the maximum amplitude at saturation is therefore helpful to choose an optimal intensity.

Limitations

The range of TMS intensities used is limited at the lower end by the motor threshold, as stimulation at intensities significantly below RMT does not result reliably in EMG responses in any brain-state. Nevertheless, sub-threshold TMS does affect cortical circuits, as can be demonstrated, for instance, in paired-pulse paradigms (e.g. Refs. [31,32]), with pre-innervation [33], or in TMS evoked EEG potentials [34,35]. It is therefore feasible (using paired-pulse protocols, performing stimulation during pre-innervation, or using cortical EEG responses) to investigate in subsequent studies whether EEG-defined brain-states can be differentiated at intensities below single-pulse RMT.

In addition to phase, pre-stimulus oscillatory power has been shown to modulate perception [36–39], but in our experimental design, the impact of instantaneous μ-power (or power in other frequency bands) on MEP amplitude is difficult to assess. As we used a power-threshold, to ensure suitable accuracy of the phase-detection algorithm, no trials with low μ-power were acquired. Real-time triggered EEG-TMS could be used in the future to explore the role of instantaneous power.

Some participants displayed very large modulation of MEP amplitudes by prestimulation activity phase, while others showed only minor or no modulation. We tried to identify factors which predict the individual degree of phase-modulation. High SNR alone is not sufficient for a large effect, as in our data set, there are participants with high SNR but no modulation of MEP amplitude by μ-phase. Furthermore, the standard Laplacian C3 filter may not extract the functionally relevant oscillatory component, depending on individual anatomical features. The large variability between the degree of observed phase-modulation raises the question if improved demixing of EEG-signals could aid in uncovering the latent effect of prestimulation phase on variability of MEP amplitudes in participants showing no phase-modulation in the present study. Future studies may improve this aspect by using individualized spatial filters or anatomically guided source level analysis. This may also increase the proportion of participants which can be studied with phase-dependent brain stimulation, as in this study only participants with a μ-rhythm as detected by a standard C3 Hjorth montage were included, whereas individualized approaches will yield increased SNR for oscillatory components.

The conditions required to establish a clear dependence of cortical excitability on instantaneous μ-phase are not sufficiently understood yet. Understanding this dependence will yield a clearer view on what exactly is stimulated by TMS, and on the interplay of endogeneous oscillatory rhythms in motor areas and their functional role.

Declarations of interest

None.

Acknowledgements

We thank Anna Kempf and Tamara Vasilkovska for help with participant coordination and experimental preparation. NS and JT acknowledge support from the Quandt foundation. NS and CZ are supported through a German Federal Ministry for Economic Affairs and Energy of EXIST Transfer of Research Grant. CZ acknowledges support from the Clinician Scientist Program at the Faculty of Medicine at the University of Tübingen. UZ acknowledges support from the German Research Foundation (DFG, grant ZI 542/7-1). This research was supported with funding from the Federal Ministry of Education and Research of Germany through the MOTOR-BIC project (BMBF, grant 13GW0053A).

Appendix A. Supplementary data

Supplementary data to this article can be found online at https://doi.org/10.1016/j.brs.2018.09.009.

References

[1] Wang XJ. Neurophysiological and computational principles of cortical rhythms in cognition. Physiol Rev 2010;90(3):1195–268.
[2] Buzsáki G, Draguhn A. Neuronal oscillations in cortical networks. Science 2004;304(5679):1926–9.
[3] VanRullen R, Busch NA, Drewes J, Dubois J. Ongoing EEG phase as a trial-by-trial predictor of perceptual and attentional variability. Front Psychol 2011;2(60):1–9.
[4] Fries P. A mechanism for cognitive dynamics: neuronal communication through neuronal coherence. Trends Cognit Sci 2005;9(10):474–80.
[5] Jensen O, Mazaheri A. Shaping functional architecture by oscillatory alpha activity: gating by inhibition. Front Hum Neurosci 2010;4(4):1–8.
[6] Busch NA, Dubois J, VanRullen R. The phase of ongoing EEG oscillations predicts visual perception. J Neurosci 2009;29(24):7869–76.
[7] Mathewson KE, Gratton G, Fabiani M, Beck DM, Ro T. To see or not to see: prestimulus α phase predicts visual awareness. J Neurosci 2009;29(9):2725–32.
[8] Dugué L, Marque P, VanRullen R. The phase of ongoing oscillations mediates the causal relation between brain excitation and visual perception. J Neurosci 2011;31(33):11889–93.
[9] Ai L, Ro T. The phase of prestimulus alpha oscillations affects tactile perception. J Neurophysiol 2013;111(6):1300–7.
[10] Keil J, Timm J, SanMiguel I, Schulz H, Obleser J, Schönwiesner M. Cortical brain states and corticospinal synchronization influence TMS-evoked motor potentials. J Neurophysiol 2014;111(3):513–9.
[11] Kiers L, Cros D, Chiappa K, Fang J. Variability of motor potentials evoked by transcranial magnetic stimulation. Electroencephalogr Clin Neurophysiol 1993;89(6):415–23.
[12] Ellaway P, Davey N, Maskill D, Rawlinson S, Lewis H, Anissimova N. Variability in the amplitude of skeletal muscle responses to magnetic stimulation of the motor cortex in man. Electroencephalogr Clin Neurophysiol 1998;109(2):104–13.

[13] Berger B, Minarik T, Liuzzi G, Hummel FC, Sauseng P. EEG oscillatory phase-dependent markers of corticospinal excitability in the resting brain. BioMed Res Int 2014, 936096.
[14] Mäki H, Ilmoniemi RJ. EEG oscillations and magnetically evoked motor potentials reflect motor system excitability in overlapping neuronal populations. Clin Neurophysiol 2010;121(4):492–501.
[15] van Elswijk G, Maji F, Schoffelen J-M, Overeem S, Stegeman DF, Fries P. Corticospinal beta-band synchronization entails rhythmic gain modulation. J Neurosci 2010;30(12):4481–8.
[16] Zrenner C, Desideri D, Belardinelli P, Ziemann U. Real-time EEG-defined excitability states determine efficacy of TMS-induced plasticity in human motor cortex. Brain Stimul 2018;11(2):374–89.
[17] Pineda JA. The functional significance of mu rhythms: translating "seeing" and "hearing" into "doing". Brain Res Rev 2005;50(1):57–68.
[18] Schaworonkow N, Triesch J. Ongoing brain rhythms shape I-wave properties in a computational model. Brain Stimul 2018;1(4):828–38. https://doi.org/10.1016/j.brs.2018.03.010.
[19] Nikulin VV, Brismar T. Phase synchronization between alpha and beta oscillations in the human electroencephalogram. Neuroscience 2006;137(2):647–57.
[20] Rossi S, Hallett M, Rossini PM, Pascual-Leone A, of TMS Consensus Group S, et al. Safety, ethical considerations, and application guidelines for the use of transcranial magnetic stimulation in clinical practice and research. Clin Neurophysiol 2009;120(12):2008–39.
[21] Rossini P, Burke D, Chen R, Cohen LG, Daskalakis Z, Di Iorio R, et al. Non-invasive electrical and magnetic stimulation of the brain, spinal cord, roots and peripheral nerves: basic principles and procedures for routine clinical and research application. An updated report from an I.F.C.N. Committee. Clin Neurophysiol 2015;126(6):1071–107.
[22] Groppa S, Oliviero A, Eisen A, Quartarone A, Cohen L, Mall V, et al. A practical guide to diagnostic transcranial magnetic stimulation: report of an IFCN committee. Clin Neurophysiol 2012;123(5):858–82.
[23] Hjorth B. An on-line transformation of EEG scalp potentials into orthogonal source derivations. Electroencephalogr Clin Neurophysiol 1975;39(5):526–30.
[24] Blankertz B, Acqualagna L, Dähne S, Haufe S, Schultze-Kraft M, Sturm I, et al. The Berlin brain-computer interface: progress beyond communication and control. Front Neurosci 2016;10.
[25] Siebner HR, Hartwigsen G, Kassuba T, Rothwell JC. How does transcranial magnetic stimulation modify neuronal activity in the brain? Implications for studies of cognition. Cortex 2009;45(9):1035–42.
[26] Thickbroom GW. A model of the contribution of late I-waves to mu-motoneuronal activation: implications for paired-pulse TMS. Brain Stimul 2011;4(2):77–83.
[27] Ikoma K, Samii A, Mercuri B, Wassermann E, Hallett M. Abnormal cortical motor excitability in dystonia. Neurology 1996;46(5):1371–2.
[28] Devanne H, Lavoie B, Capaday C. Input-output properties and gain changes in the human corticospinal pathway. Exp Brain Res 1997;114(2):329–38.
[29] Di Lazzaro V, Oliviero A, Profice P, Pennisi M, Pilato F, Zito G, et al. Ketamine increases human motor cortex excitability to transcranial magnetic stimulation. J Physiol 2003;547(2):485–96.
[30] Lücke C, Heidegger T, Röhner M, Toennes SW, Krivanekova L, Müller-Dahlhaus F, et al. Deleterious effects of a low amount of ethanol on LTP-like plasticity in human cortex. Neuropsychopharmacology 2014;39(6):1508–18.
[31] Kujirai T, Caramia MD, Rothwell JC, Day BL, Thompson PD, Ferbert A, et al. Corticocortical inhibition in human motor cortex. J Physiol 1993;471:501–19.
[32] Ziemann U, Rothwell JC, Ridding MC. Interaction between intracortical inhibition and facilitation in human motor cortex. J Physiol 1996;496:873–81.
[33] Di Lazzaro V, Restuccia D, Oliviero A, Profice P, Ferrara A, Insola A, et al. Effects of voluntary contraction on descending volleys evoked by transcranial stimulation in conscious humans. J Physiol 1998;508(2):625–33.
[34] Komssi S, Kähkönen S, Ilmoniemi RJ. The effect of stimulus intensity on brain responses evoked by transcranial magnetic stimulation. Hum Brain Mapp 2004;21(3):154–64.
[35] Fecchio M, Pigorini A, Comanducci A, Sarasso S, Casarotto S, Premoli I, et al. The spectral features of EEG responses to transcranial magnetic stimulation of the primary motor cortex depend on the amplitude of the motor evoked potentials. PLoS One 2017;12(9).
[36] Hanslmayr S, Aslan A, Staudigl T, Klimesch W, Herrmann CS, Bäuml KH. Prestimulus oscillations predict visual perception performance between and within subjects. Neuroimage 2007;37(4):1465–73.
[37] Van Dijk H, Schoffelen JM, Oostenveld R, Jensen O. Prestimulus oscillatory activity in the alpha band predicts visual discrimination ability. J Neurosci 2008;28(8):1816–23.
[38] Linkenkaer-Hansen K, Nikulin VV, Palva S, Ilmoniemi RJ, Palva JM. Prestimulus oscillations enhance psychophysical performance in humans. J Neurosci 2004;24(45):10186–90.
[39] Weisz N, Wühle A, Monittola G, Demarchi G, Frey J, Popov T, et al. Prestimulus oscillatory power and connectivity patterns predispose conscious somatosensory perception. Proc Natl Acad Sci 2014;111(4):E417–25.